Numerical Study to Evaluate the Effect of Ductile Element in the Seismic Performance of Steel Frames with EBF

S. Reza Salimbahrami[1] · M. Naghipour[2]

Abstract

This paper presents the results of a numerical study, using ANSYS and OpenSees, of Ductile Element in the Seismic Performance of Steel Frames with eccentrically braced frame. This ductile element as dissipater includes a ring with a box around it that increases the ductility and energy dissipation of structures during an earthquake strike. It can be installed in every brace frame. Furthermore, during an earthquake, it contributes a significant portion of dissipated input energy by entry into the non-linear phase. Additionally, flexural plastic hinges are formed. With this, the entrance of other members to the non-linear phase is postponed. As a result, the buckling of the brace members is prevented. The box increases the capacity of the ductile members. The increase in the ring diameter and thickness results in a reduced ductility rate. Using a non-linear finite element analysis, the stresses and deformations under cyclic load are studied. The obtained hysteresis curves indicate that the element can act as an energy dissipating member, as well as a fuse to control the buckling of a brace. Moreover, this member can increase ductility in structures. Additionally, the operation of the ductility element in 2D eccentrically brace frames is considered. The non-linear time history analysis is conducted by OpenSees. The achieved results showed a decrease in the base shear and rotation of the link beam and an increase in ductility.

Keywords Eccentrically braced frames · Replaceable energy dissipation device · Ductile element · Numerical simulation · Nonlinear seismic performance

1 Introduction

Among all earthquakes resistant structural systems, flexural frames in particular, are considered to be a good lateral load bearing system. They have high ductility and low stiffness. However, it is different for braced frames. While the concentrically braced frames (CBF) are stiff, their ductility is not adequate. On the other hand, Eccentrically Braced Frames (EBF) have a good balance of stiffness and lack of ductility. In this type of structural system, the essential role of absorption and dissipation of induced energy is played by a link beam. Due to an opening or a door next to a column, in some configurations of Eccentrically Braced Frames, it is necessary to connect a link beam to a column. The

earthquake in Northridge (1994) marked the beginning of a series of important studies regarding flexural frame connections. As a result of this earthquake, many seismic design codes of flexural frames were revised and research on the link beam to column connections were carried out. The link beam bears great forces and large inelastic deformations in flexural joints. Thus, after the Northridge earthquake, it was necessary to suggest a good strategy to provide the required ductility of these connections.

Despite the studies conducted by Okazaki (2004) and Drolias (2007), as well as the surveys carried out by Prinz and Richards (2009) and Bremen et al. (2010), until now, any appropriate and satisfactory connection between link beam and column have been proposed by design codes. In the seismic criteria of AISC (2005), due to ongoing research to overcome the drawbacks of this type of connection, designers are recommended not to use this type of connection. Hence, the importance of studying beam-to-column connections in diverge braced systems has become more essential.

Based on the studies conducted on the ductile element, Kafi et al. (Abbasnia et al. 2009) took a step towards

✉ S. Reza Salimbahrami
  salimbahrami@semnan.ac.ir

1 Technical and Vocational University, Sari, Iran

2 Department of Civil Engineering, Babol Noshirvani University of Technology, Babol, Iran

improving the convergent brace by introducing a ductile ring. Analytical results by Andalib et al. (2018), Mohammad Bazzaz et al. (2012, 2014, 2015a, b); Bazzaz et al. (2011); revealed that the performance of steel ring studied as a ductile element in an off-centre bracing system (model off-centre braced frame and ductile element in optimum place) has more ductility among the models. Also Andalib et al. (2014) investigated the ductility and performance of steel rings constructed from plates. The results of this investigation show that the hysteresis curve of the steel specimen made of steel plates is wide and that a tensile ductility factor of 8.68 is achieved.

Also, experimental and numerical evaluation of an innovative diamond-scheme bracing system equipped with a yielding damper by Pachideh et al. (2020) indicated that both great applicability and efficiency of the proposed system in energy absorption and ductility. Moreover, it was concluded that as the braces and damper are in parallel, the use of a steel ring with smaller size and thickness would result in higher energy absorption and load-resisting capacity when compared to the other existing systems. Kheyroddin et al. (2019) assessed the RC frames retrofitted by steel jacket, X-brace and X-brace having ductile ring as a structural fuse. They found that although the frame retrofitted by the X-brace showed a better performance in terms of resistance and stiffness, but the retrofitted frame with a ring also showed a better behaviour in terms of resistance and stiffness compared to the RC frame and the sample with the jacket as well as compared to the sample with the X-brace showed more ductility and energy dissipation (with a slight reduction in resistance).

The concentrically braced frames (CBFs) are one of the most widely used lateral load-resisting systems. Kachooee et al. (2018a, b) evaluated the effect of local fuse on behaviour of concentrically braced frame by a numerical study. They found that if the reduced cross-section fuse (RCF) is properly designed and also the end of brace is fixed, the CBFs with equal energy dissipation capacity, that are equipped with this fuse exhibit a better ductility than the customary CBFs. Also Rahnavard et al. (Naghavi et al. 2019; Rahnavard et al. 2017, 2020) did some research on brace. Results of Rahnavard et al. indicated dramatic improvements in energy dissipation and ductility in BRBF models as compared to equivalent CBF models.

Experimental and numerical evaluation of Y-shaped eccentrically braced frames fabricated with high strength steel by Mingzhou et al. (Lian et al. 2015; Liang et al. 2018a, b; Ling et al. 2019) indicated that the one-bay and one-story Y-HSS-EBF specimen had good load-bearing capacity and ductility capacity. Also, Results from the simplified analysis were compared with the test results. The test results indicated that the specimen had reliable lateral stiffness and the damages observed at shear links.

This study attempts to develop a model of energy dissipater. It consists of a ring that increases the ductility and earthquake energy absorption. Additionally, a box joined to the ring by a connection plate increases the bearing capacity. During an earthquake, a considerable portion of the energy is absorbed by the dissipater which its behaviour has transformed into non-linear and flexural plastic hinges were formed. This way, the non-linear stage of other members is prevented. Furthermore, the buckling of bracing member and the failure of the link beam are also postponed or avoided. If the proposed element fails, it can be easily replaced. In addition to its low cost, the speed of its implementation is also high. It is predicted that the proposed element can act as a dissipater member and also as a fuse for controlling the buckling of the brace and rotation of link beam. Thus, it provides sufficient ductility for the system.

2 The Research Method

This research was conducted in two phases. In the first phase, the behaviour of the different proposed elements is simulated and the optimum element is selected in accordance with the obtained results. The results of this phase were used to evaluate the behaviour of the EBF in the next phase. To select the optimum element, 15 types of proposed elements are evaluated. These differed in terms of ring and box dimensions. Furthermore, the parameters required to evaluate the behaviour of the proposed element of finite element analysis in cyclic loading are introduced.

In the second phase, the effect of using the proposed element in EBF is investigated. For this purpose, the EBFs are simulated with the proposed element, as well as without it. This is carried out in OpenSees. It is important to note that, in this study, EBF is used for the usual EBF and D-EBF is used for EBF with ductile element. The seismic performance of EBF using a non-linear dynamic analysis is evaluated according to time history. Then the results are compared. The effect of this element was also investigated in four, six and eight story frames. Figure 1 shows the placement of the element in a braced frame. It is important to note that the proposed element was joined to the brace by a welding or screw.
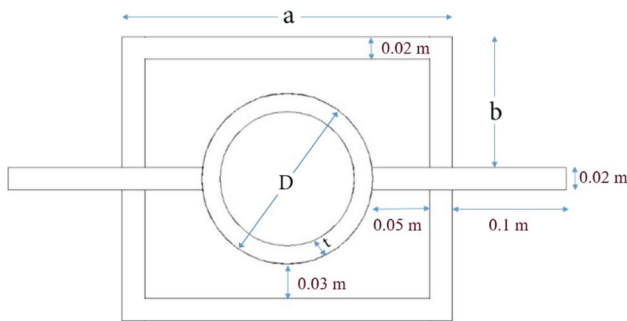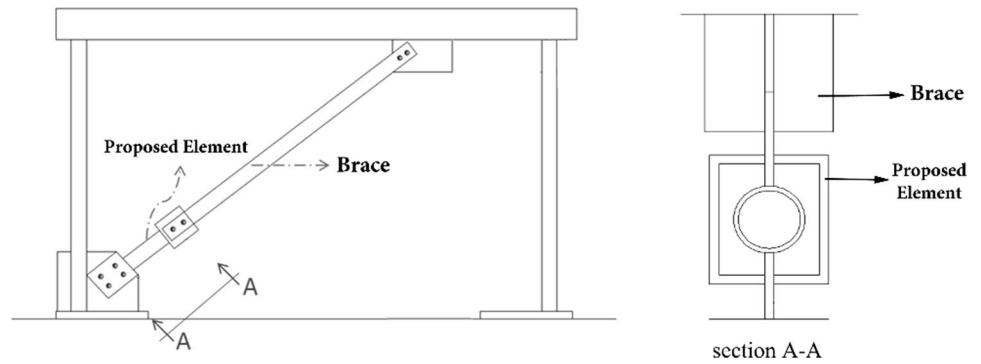
3 The Research Process

3.1 Phase One: Analysing the Proposed Element

3.1.1 Introducing the Proposed Element

Figure 2 shows the proposed element. This was composed of a ring and two plates, adjoining the ring to the two half

Fig. 1 The position of proposed element in EBF (Salimbahrami 2013)

section A-A

Fig. 2 Proposed element dimension (Salimbahrami 2013)

boxes. D, L, and t are the diameter, the length and the thickness of the ring, respectively. The plates dimensions were $0.17 \times 0.1 \times 0.02$ m.

In this study, 15 models are considered for the proposed element. The difference in these models was the dimension of ductile steel rings. These consisted of three types of dimensions (0.15, 0.2 and 0.25 m) and five types of thickness (0.01, 0.012, 0.014, 0.016 and 0.018 m). In all of the elements, the length of the ring was 0.1 m. The dimension of the box changed proportionally to the ring diameter. Figure 2 shows the parametric dimension of the element. Parameters a, b, D, and t in Fig. 2 for 15 models are presented in Table 1.

One of the effective parameters for steel ring selection is steel properties. Since the role of the ring is energy dissipation, ductility becomes an important property of this ring. Thus, it is recommended to choose soft steel with high ductility. Soft steel is a type of steel with a yielding stress of less than 305,914,863.89 kg/m². Its ultimate strain is more than 40%. Thus, taking the market into consideration, a seamless steel pipe CT20 for the ring is selected. Although this steel does not have the property of soft steel, for the evaluation of the performance of the proposed element in this phase, it is a good choice (Abbasnia et al. 2009). For the plates that join the brace to the box, St37 is used. The mechanical properties of all members of the element, such as ultimate stress and strain, yielding stress and elastic modulus, are given in Table 2.

Table 1 The dimensions of various types of the proposed elements

| Sample	D (m)	t (m)	a (m)	b (m)
DE[a]-15–1	0.15	0.01	0.29	0.115
DE-15–1.2	0.15	0.012	0.29	0.115
DE-15–1.4	0.15	0.014	0.29	0.115
DE-15–1.6	0.15	0.016	0.29	0.115
DE-15–1.8	0.15	0.018	0.29	0.115
DE-20–1	0.2	0.01	0.34	0.14
DE-20–1.2	0.2	0.012	0.34	0.14
DE-20–1.4	0.2	0.014	0.34	0.14
DE-20–1.6	0.2	0.016	0.34	0.14
DE-20–1.8	0.2	0.018	0.34	0.14
DE-25–1	0.25	0.01	0.39	0.165
DE-25–1.2	0.25	0.012	0.39	0.165
DE-25–1.4	0.25	0.014	0.39	0.165
DE-25–1.6	0.25	0.016	0.39	0.165
DE-25–1.8	0.25	0.018	0.39	0.165

[a]Ductile Element

3.1.2 Modelling and Evaluating Performance of the Proposed Element

To evaluate the performance of the ductile element under earthquake cyclic load, the proposed model presented properties that were modelled three dimensionally in ANSYS, using element SOLID185. This type of element included eight nodes. Each node had three degrees of freedom (ux, uy, uz). In the proposed non-linear analyses, it showed stress, internal forces and loading in or out of the surface. Figure 3 shows the element SOLID185.

After creating the geometrical model and the meshing on it, loading on the 0.1 m on the junction plate to the brace was performed. A measurement of 0.1 m is chosen, as this is more adaptive to a real loading condition. At one end of the proposed element, all degrees of freedom were restrained. At the other end, all degrees of freedom were restrained in the elements except the one in the horizontal axis. The loading protocol was based on ATC24

Table 2 Mechanical properties of the component of the element

	Elastic Modulus (kg/m^2)	Poisson's ratio v	Ultimate Strain ε_U	Yielding Stress F_y (kg/m^2)	Ultimate Stress F_u (kg/m^2)
Ring	20,000,000,000	0.3	0.21	30,000,000	48,000,000
St37	21,000,000,000	0.3	0.26	24,000,000	37,000,000
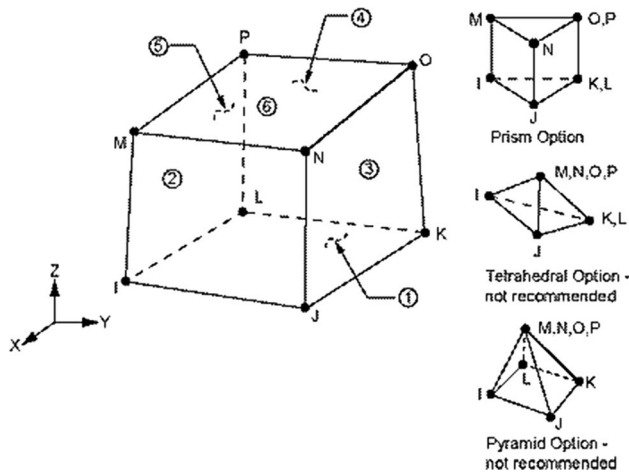
Fig. 3 The geometry of the element SOLID185 (Stolarski et al. 2018)
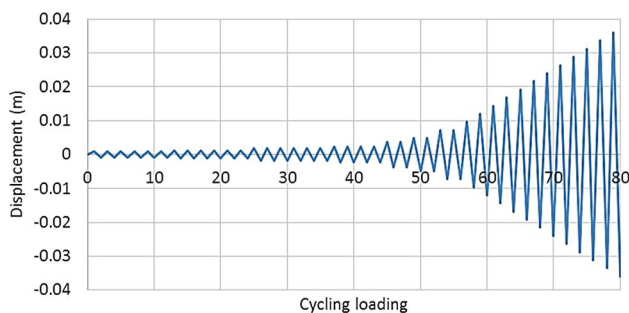
Fig. 4 Cyclic Loading in code ATC 24 (Krawinkler 1992)

(Krawinkler 1992) and was unrestrained at the end of the element. This type of loading was cyclic along the horizontal axis. The diagram of this cyclic load is shown in Fig. 4. Finally, the non-linear static model is analysed.

To compare the ductility and maximum load that the element can bear, the cyclic load (shown in Fig. 5) is applied to the model. After that, the maximum allowable displacement of the ring was 0.02 m (Abbasnia et al. 2009). This was because the initial fracture sustained load decreases. With this in mind, the applied displacement is considered to the ring, shown in Fig. 5. These results established relations between ductility, maximum sustained force in the element, diameter and the thickness of the ring.
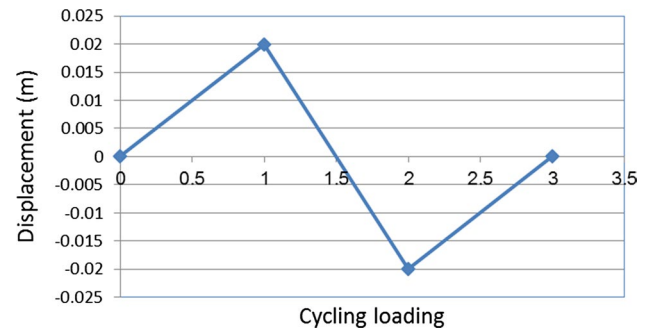
**Fig. 5** Time history loading for proposed element

3.1.2.1 Validation In order to validate the modelling in ANSYS, first, only the steel ring is simulated according to the mechanical specifications in the Table 2 with a diameter of 22, a thickness of 1.2 and a length of 10 cm according to the Fig. 6a. The steel ring is loaded with the ATC24 code as shown in Fig. 4. The loading of the rings started in cycles and started from small displacements and continued until the failure location of 2 cm. This stage of experiments was performed during four experiments to check the ductility, bearing capacity and maximum change in ring diameter. Then, these results are compared with the experimental results (Abbasnia et al. 2009) (Fig. 6b).

As can be seen in Fig. 6b, the initial stiffness of the experimental and finite element models is well matched, but as the finite element model is loaded, it goes out of linear condition sooner and surrenders in it. The similarity between the load–deflection curve in simulation and experiment showed that the simulation results were valid.

3.2 Phase Two: Static and Dynamic Analysis in EBF

3.2.1 Introducing the Samples in OpenSees

In order to evaluate the seismic performance of the proposed element, the usual structures are used. For the evaluation of the effect of the structure's height, the frames in four, six and eight stories (Fig. 7) are analysed. The height of each story was assumed 3 m and the length of each opening was 5 m. To reach an EBF with more suitable stiffness and ductility, a link beam with the shear behaviour length of e = 1 m is selected. It is considered that the dead load and

(a)

(b)
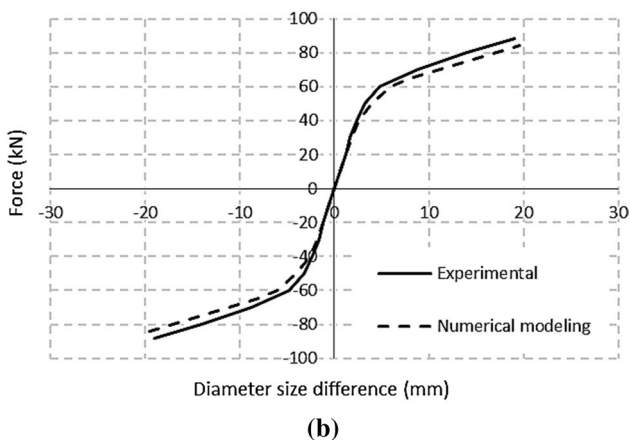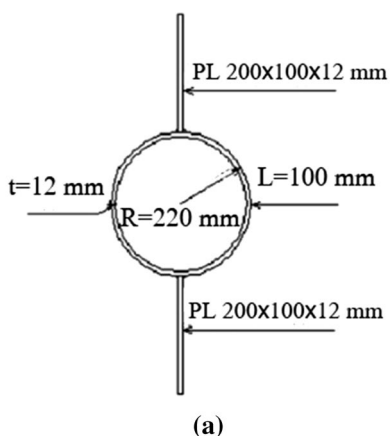
Fig. 6 **a** Geometric characteristics of experimental and numerical models **b** Comparative push plots for experimental specimen and numerical model

live load in the stories as 700 and 200 kg/m², respectively. Additionally, the effective width of frames was 3 m, as was considered in the plan of Fig. 7. Consequently, the line dead load and live load were 2100 and 600 kg/m, respectively. These were distributed along the beam. The plan of this study was uniform (square, regular, orderly and ordered) and the height of the structure was below 50 m. Thus, the equivalent static analysis are performed. Based on the sixth topic of the Iran National Building Regulations (Code 2013), the site with high risk and soil type three were chosen for the seismic coefficient of the structure. The seismic properties static analysis were relevant to Iran 2800 code (Code 2014) and are shown in Table 3.

3.2.2 Analysis and Design Parameters

All of the frames were designed based on the tenth topic of the Iran National Building Regulations (edition 2008) (Code 2014). For the analysis and design of the frames, ETABS (Berkeley 2015) is used. Furthermore, the UBC (1997) (UBC 1994) was used as the basis for designing. The seismic design criterion in the tenth topic of the Iran National Building Regulations (edition 2008) (Code 2014) has a number of similarities to the seismic design criterion in this code. The properties of the sections of columns and beams for four, six and eight story frames are considered as they are shown in Table 4. Previous studies have shown that the probability of brittle failure in the side link beam to the weak axis of the column is high. Thus, this type of joint has not been used.

(a)

(b)

(c)
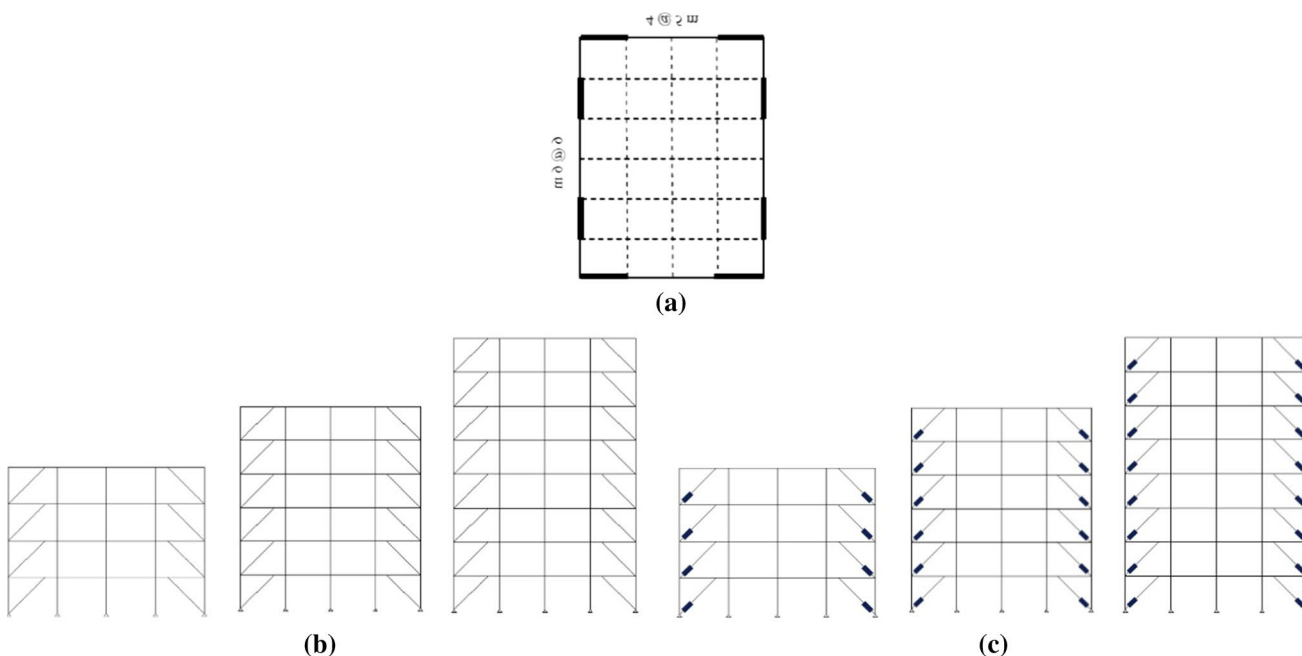
Fig. 7 EBF in 4, 6, and 8 stories **a** Plan **b** EBF **c** D-EBF

Table 3 Seismic properties of static analysis based on Iran 2800 Code

Story	A	T	I	R	B	C
4	0.35	0.322	1	7	2.75	0.1375
6	0.35	0.437	1	7	2.75	0.1375
8	0.35	0.542	1	7	2.75	0.1375

Table 4 Section properties in EBF

Story	Section					
	4-story		6-story		8-story	
System	EBF	D-EBF	EBF	D-EBF	EBF	D-EBF
Column	IPB400	IPB400	2IPB300	2IPB300	2IPB500	2IPB500
Beam	2IPE300	2IPE300	2IPE300	2IPE300	2IPE300	2IPE300
Brace	2UNP220	2UNP220 + DE-15–1.8	2UNP240	2UNP240 + DE-15–1.8	2UNP220	2UNP220 + DE-15–1.8

Table 5 Properties of selected accelerometer records

Record	Year	Station	Magnitude	PGA[a] (g)	Distance to fault rupture (km)	Site
Imperial Valley	1979	Chihuahua	6.53	0.27	28.7	3
Tabas	1978	Boshroyeh	7.35	0.108	26.1	3
Northridge	1994	Canoga	6.69	0.46	37.9	3

[a]Peak ground acceleration

3.2.3 Accelerometer

Accelerometers are used to determine the displacement of the earth. These should be as close as the real displacement of the earth in earthquake in the place that the structure constructed. In this study, the accelerometers are using parameters such as shear wave velocity in the soil where the accelerometer records, the distance of the accelerometers to the fault and the frequency content. As shown in Table 5, three accelerometers are chosen based on code 2800. These accelerometers had the following three features:

- Their shear wave velocity was in a range that was based on code 2800 (the soil could be classified as type three).
- They were far from fault and
- They had a wide range of frequency content in the district of structure period inclusion.

These accelerometers were for earthquakes in Imperial Valley, Tabas and Northridge.

3.2.4 Procedure of Modelling in OpenSees

EBF with the proposed element and without it was modelled in 2D (Fig. 8). It was modelled in OpenSees (Mazzoni
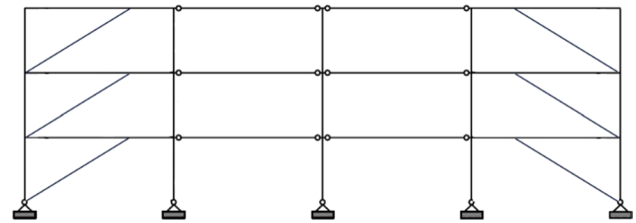
Fig. 8 Input model in OpenSees

et al. 2006). The modelling of the columns and beams was used from the non-linear beam-column element with non-elastic fibre sections. For beams, columns and braces, the Giuffer-Menegotto-Pinto (Menegotto 1973) material is exploited. This had isotropic strain stiffening, yielding stress of 24,000,000 kg/m^2 and the tangential modulus of 2.1e10 kg/m^2 (steel 02 with $F_y = 24,000,000$ kg/m^2). The proposed element was also modelled with the same material (steel 02) with regard to the relations between the force in the brace and its dimension, yielding stress and elastic model. This was concluded from the behaviour of the proposed element in ANSYS. The yielding stress and the elastic modulus of the ring with the diameter of 0.18 m and thickness of 0.012 m were 29,585,000 and 19,400,000,000 kg/m^2, respectively. It is important to note that the bearings of frames were considered as hinge.

For validation of the OpenSees model, the vibration modes resultant of modal analysis in SAP (SAP 2005) are compared with OpenSees for a four story (Fig. 8). The validation of the OpenSees model is presented in Table 6. To model the link beam in EBF, the assumed method of Remdan and Ghobarah (1995) is used, along with the modification by Richard (Richards 2004). According to Table 6, there is a good correlation between the results of SAP and OpenSees.

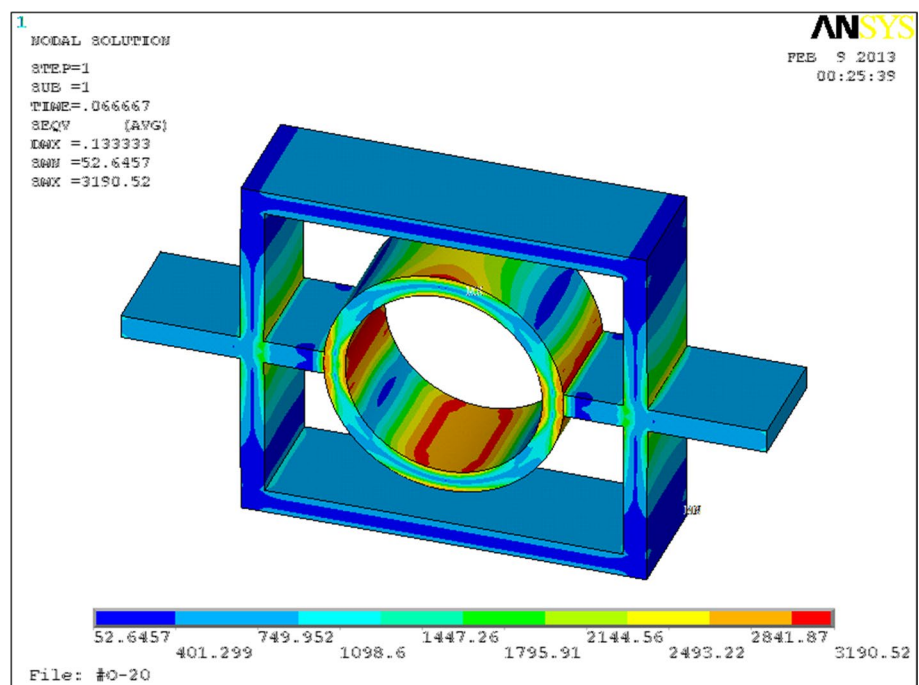### 3.3 Results of Modelling of the Proposed Element in ANSYS

3.3.1 Von Misses Stress Distribution in the Proposed Element

It is demonstrated that the Von Misses Stress Distribution in the proposed element with one cycle loading, as seen in Fig. 9. The inner stress of the ring was greater than the outer one. Thus, failure initiating from the inner part and extending outwards is anticipated. As the metals were weaker, the failure most likely occurred when the ring was under pressure and the inner part carried maximum compression stress.

3.3.2 The Sustainable Force and the Amount of Energy Dissipation by the Proposed Element
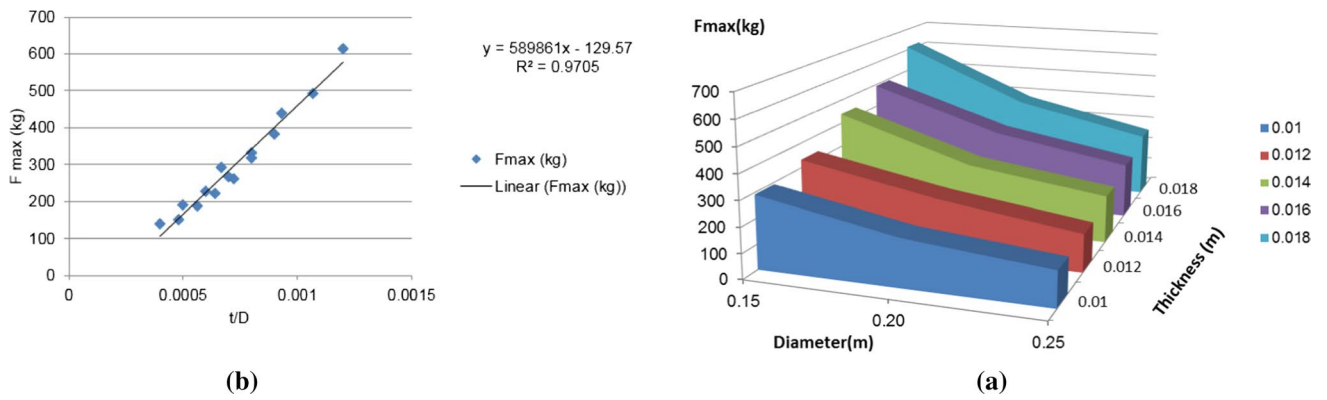
Figures 10 and 11 show the relations between the exerted force and energy dissipation in the proposed element. This is with regard to the thickness to diameter ratio and exerted force and the energy dissipation diagram in the proposed element for the 15 modelled elements with the mentioned dimension. A second order regression (Figs. 10a and 11a) is used to achieve good relations between the sustainable force and energy dissipation in the proposed element, with respect to the thickness to diameter ratio. Figures 10b and 11b show that, by decreasing the ring diameter and increasing its thickness, the amount of force and energy dissipation increases.

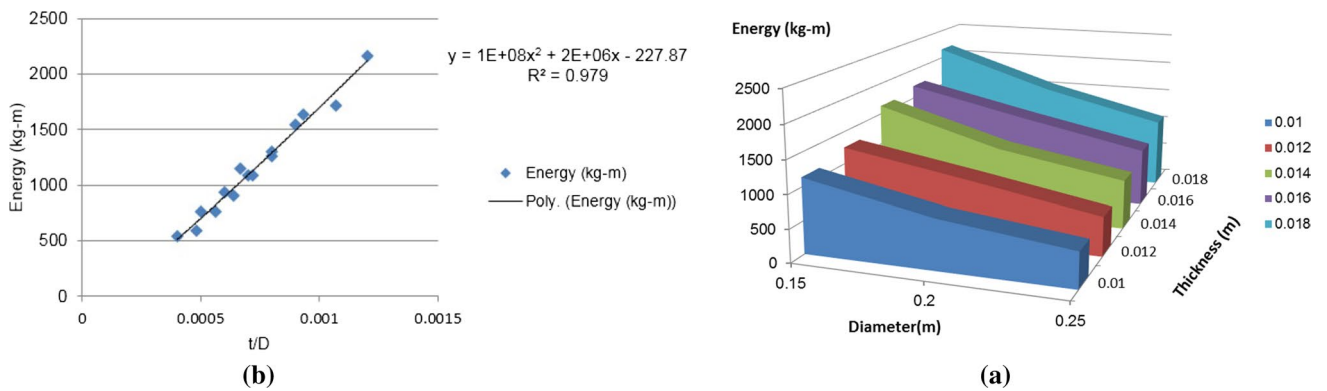#### 3.3.3 Force Response Curve to the Displacement in the Proposed Element

Figure 12 shows the force response curve to the displacement of the proposed element. Taking this figure into consideration, one could argue that the proposed element has the same performance in compression and tension. This suggests that the model is reliable.

3.3.4 The Hysteresis Curve of the Proposed Element

Figure 13 shows the hysteresis curve for one sample of the proposed element with the diameter 0.15 m and thickness of 0.18 m. As illustrated in this figure, the curve for this sample

Table 6 The comparison of vibration mode between SAP and OpenSees

	OpenSees	SAP
T_1	0.278233	0.278228
T_2	0.10117	0.10117
T_3	0.060344	0.060341

Fig. 9 Von misses stress distribution in proposed element

y = 589861x - 129.57
R² = 0.9705

(b)   **(a)**

**Fig. 10** **a** The relation between applicable Force in element and portion of thickness to diameter **b** the diagram of applicable force in proposed element

y = 1E+08x² + 2E+06x - 227.87
R² = 0.979

(b)   **(a)**

Fig. 11 **a** The relation between energy dissipation and the portion of thickness to diameter **b** The diagram of applicable energy dissipation in proposed element
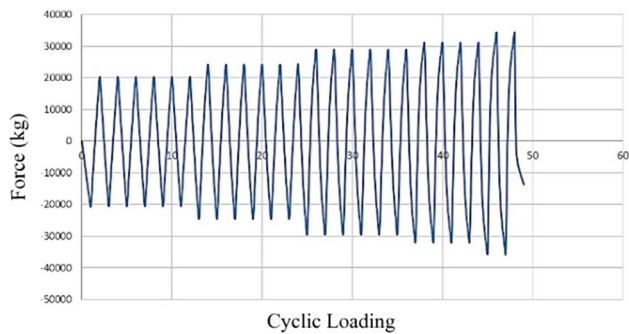
Fig. 12 Force response to the displacement in proposed element
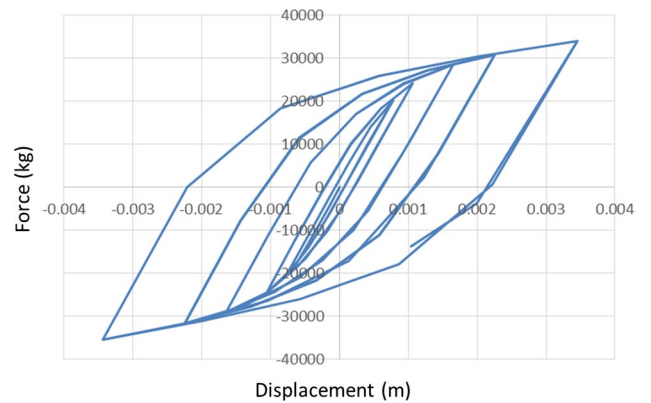
Fig. 13 Hysteresis curve for proposed element

is wide and regular. This hysteresis curve indicates that the model dissipates energy efficiently.

3.4 Results of the Non-linear Dynamic Analysis of the EBF in the Form of Time History

3.4.1 Maximum Relative Lateral Displacement in Stories

Figure 14 shows the maximum relative lateral displacement in stories of the frames with EBF and D-EBF under Imperial Valley, NorthRidge, and Tabas earthquakes. The relative lateral displacement of the stories is an important and sensitive factor in the performance evaluation of structure. This is due to the amount of inserted damage to the structural and non-structural part in each story which is directly related to it. Consequently, this parameter can be considered as an index of damage. The achieved results indicate that the relative displacement in most of the stories decreased and, therefore, can reduce the amount of damage to the structures. The reduction in lateral displacement begins from the second story.

3.4.2 Plastic Rotation in the Link Beam

Figure 15 shows the non-elastic measured rotation angle of the link beam in D-EBF, under the Imperial Valley, Northridge and Tabas earthquakes. By comparing and contrasting the results of maximum relative displacement in stories with

plastic rotation of link beam, it is examined that the non-elastic rotation angle of link beam in structure level is very similar to the maximum relative displacement of each story in structure level. Thus, the relative displacement of each story can be considered as damage index.

3.4.2.1 Maximum Base Shear and Last Story Displacement Table 7 shows the maximum base shear and last story displacement in D-EBFs under the Imperial Valley, Northridge and Tabas earthquakes.

The existence of the proposed element in EBF led to a decrement in base shear of about 55%. This is compared to EBF and results in construction cost reduction, improving the foundation of the structure and the displacement reduction of the last story of approximately 10%.

3.4.2.2 Shear Amount of Link Beam Figure 16 shows the maximum shear force of the link beam of stories. The existence of the proposed element led to a reduction of shear force in the link beam.

4 Conclusion

Studies on Eccentrically Braced Frames show that using ductile element acts like a fuse and decreases the rotation of the link beam. The results of this research are as follows.
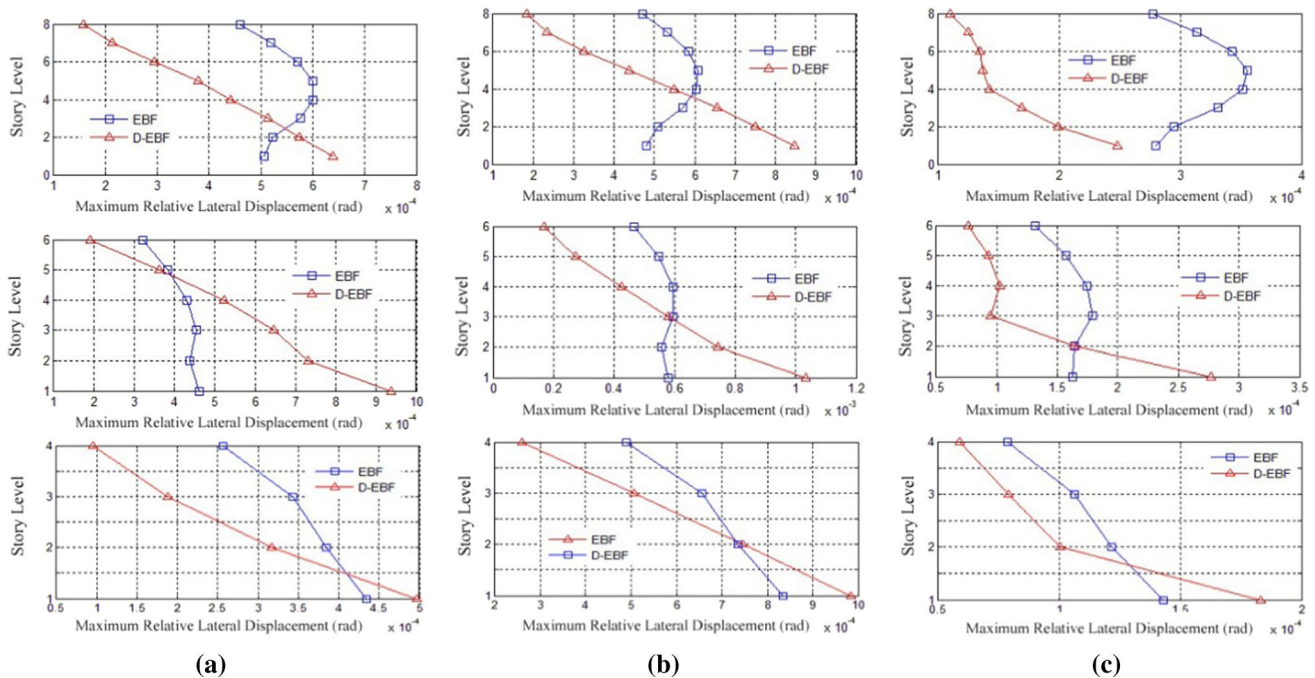

Fig. 14 Maximum relative displacement under earthquake for EBF and D-EBF in stories **a** Imperial Valley **b** Northridge **c** Tabas
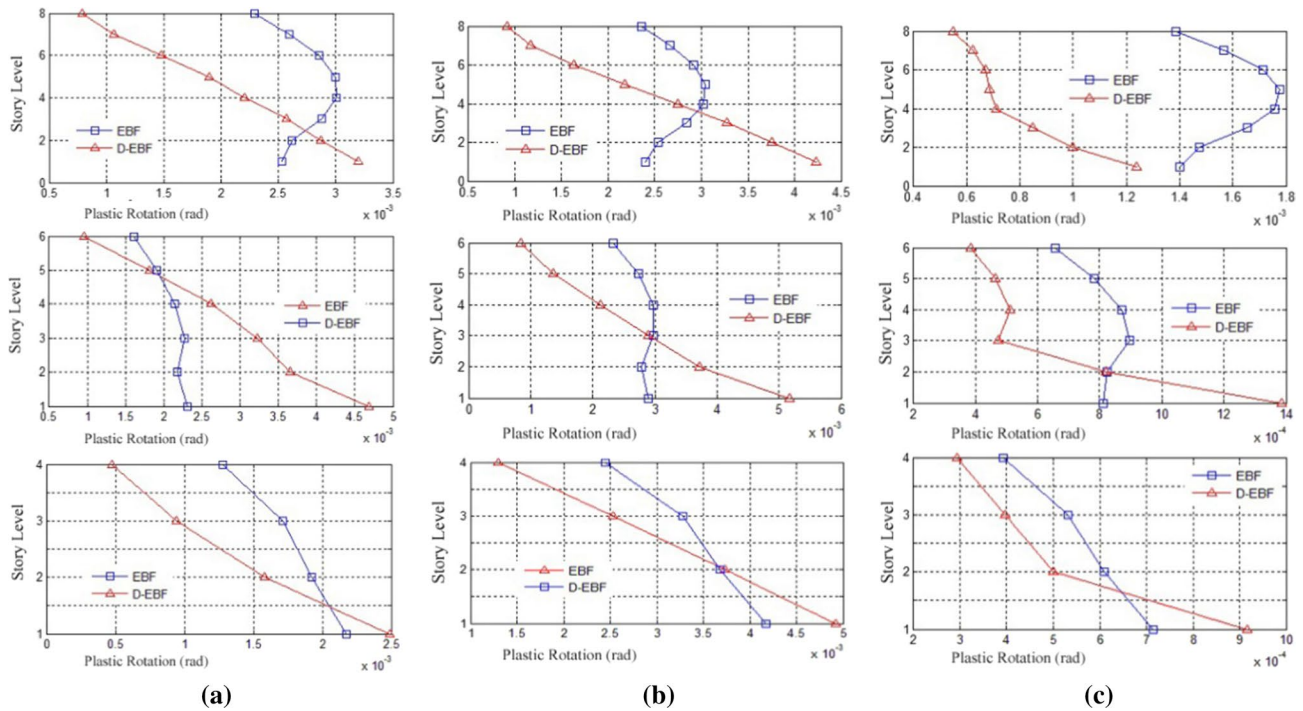
Fig. 15 Non-Elastic measured rotation angle of the link beam in EBF and D-EBF **a** Imperial Valley **b** Northridge **c** Tabas

Table 7 Comparison of maximum base shear and roof displacement in EBF and D-EBF

System	EBF		D-EBF			
Record	Base shear (kg)	Maximum roof displacement (m)	Base shear (kg)	Maximum roof displacement (m)	Difference Base Shear (%)	Difference Maximum roof displacement (%)
4-story						
Imperial Valley	29,708.59	0.0042	11,171.44	0.0032	− 62.39	− 24.84
Northridge	57,730.61	0.00814	16,237.27	0.0074	− 71.87	− 8.69
Tabas	10,240.519	0.00135	7161.987	0.0012	− 30.06	− 10/43
Average					− 54.77	− 14.65
6-story						
Imperial Valley	32,871.273	0.00742	14,733.88	0.00986	− 55.17	32.97
Northridge	41,655.329	0.010544	14,903.662	0.00953	− 64.2	− 9.57
Tabas	11,204.27	0.00290	8169.528	0.00259	− 27.1	− 10.8
Average					− 48.82	− 4.19
8-story						
Imperial Valley	39,246.3039	0.0144	15,377.858	0.01403	− 60.8	− 2.65
Northridge	41,580.714	0.01311	13,717.148	0.01178	− 67	− 10.1
Tabas	19,196.356	0.00757	8254.794	0.00358	− 56.9	− 52.7
Average					− 61.6	− 21.8
The mean difference					− 55.07	− 10

A. **Analysis Result of the Proposed Element**

- It is possible to increase the capacity of the ductile ring element using the proposed element. It is also expected that this element can dissipate a great amount of plastic energy.

- The amount of bearing force and energy dissipation increase as the diameter of the steel ring decreases.
- Since the maximum applied load to brace is equal to the maximum bearing force of the proposed element, the
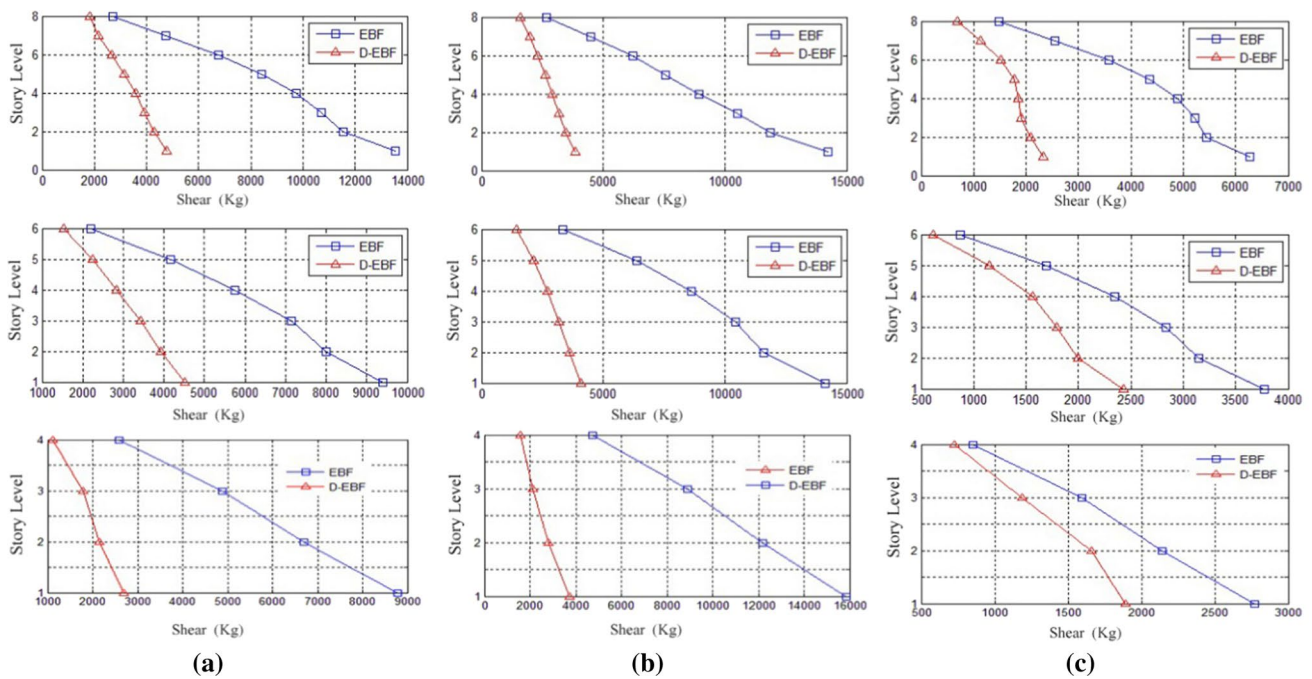
Fig. 16 Maximum sheer force of link beam in EBF and D-EBF under **a** Imperial Valley **b** Northridge **c** Tabas

element can be designed in a way to ensure that buckling does not occur.

- The relationship between the bearing force of the proposed element and the amount of dissipated energy with a regression of 99% was achieved. This is efficient for design purposes.

B. Dynamic Analysis Result of the Eccentrically Braced Frames

- Due to the relations between damage rate structural and non-structural members to relative displacement rate in stories, obtained results show a reduction in the maximum relative displacement in the stories with yielding rings in the D-EBFs. This trend occurs from the second to the last story.
- The rotation of the link beam with the proposed element in D-EBFs in the last stories decreases considerably. This highlights the importance of the dissipation energy of the proposed element.
- The amount of base shear in D-EBF including the yielding rings is about 55% of EBF.
- The displacement rate in the D-EBF including the yielding rings is about 10% of EBF.
- The existence of the proposed element leads to a reduction in the bearing shear force in the link beam in D-EBF.

To approach the modelling of the structure with eccentrically brace frame and considering all the items of the regulations, It is recommended that the structure in this research be modelled in 3D and its results with Compare the results of 2D modelling.

Also in this research, the proposed element is located in a place between the beam-to-column connection plate and the brace. Therefore, it is suggested that research be done on the location of the proposed element in a frame with EBF.

References

Abbasnia, R., Vetr, M. G., Ahmadi, R., & Kafi, M. A. (2009). An analytical and experimental study on the ductility of steel rings. *Sharif Journal of Civil Engineering, 25*(51.1), 41–48.

Andalib, Z., Kafi, M. A., Kheyroddin, A., & Bazzaz, M. (2014). Experimental investigation of the ductility and performance of steel rings constructed from plates. *Journal of Constructional Steel Research, 103,* 77–88.

Andalib, Z., Kafi, M. A., Kheyroddin, A., Bazzaz, M., & Momenzadeh, S. (2018). Numerical evaluation of ductility and energy absorption of steel rings constructed from plates. *Engineering Structures, 169,* 94–106. https://doi.org/10.1016/j.engstruct.2018.05.034.

Bazzaz, M., Andalib, Z., Kafi, M. A., & Kheyroddin, A. (2015a). Evaluating the performance of OBS-CO in steel frames under monotonic load. *Journal of Earthquakes and Structures, 8*(3), 697–710.

Bazzaz, M., Andalib, Z., Kheyroddin, A., & Kafi, M. A. (2015b). Numerical comparison of the seismic performance of steel rings in off-centre bracing system and diagonal bracing system. *Journal of Steel and Composite Structures, 19*(4), 917–937.

Bazzaz, M., Kafi, M. A., Kheyroddin, A., Andalib, Z., & Esmaeili, H. (2014). Evaluating the seismic performance of off-centre bracing system with circular element in optimum place. *International Journal of Steel Structures, 14*(2), 293–304.

Bazzaz, M., Kheyroddin, A., Kafi, M., & Andalib, Z. (2011). Evaluating the performance of steel ring in special bracing frame. In *Proceedings of the 6th International Conference of Seismology and Earthquake Engineering, 2011*

Bazzaz, M., Kheyroddin, A., Kafi, M. A., & Andalib, Z. (2012). Evaluation of the seismic performance of off-centre bracing system with ductile element in steel frames. *Steel & Composite Structures, 12*(5), 445–464.

Berkeley, C. S. I. (2015). *Computer program ETABS ultimate 2015.* Berkeley, California: Computers and Structures Inc.

Berman, J. W., Okazaki, T., & Hauksdottir, H. O. (2010). Reduced link sections for improving the ductility of eccentrically braced frame link-to-column connections. *Journal of Structural Engineering, 136*(5), 543–553.

Code, I. N. B. (2013). Applied Loads on Buildings, Part 6. Ministry of Roads & Urban Development. Tehran, Iran.

Code, I. S. (2014). Iranian code of practice for seismic resistant design of buildings 2800 (2014). Ministry of Roads & Urban Development. Tehran, Iran.

Drolias, A. (2007). Experiments on link-to-column connections in steel eccentrically braced frames (Doctoral dissertation). The University of Texas atAustin. USA.

Kachooee, A. (2018). Local fuse for improving concentric braces behavior. *Engineering and Construction Magazine* 6(82)

Kachooee, A., Kafi, M. A., & Gerami, M. (2018). The effect of local fuse on behavior of concentrically braced frame by a numerical study. *Civil Eng J, 4*(3), 655–667.

Kheyroddin, A., Sepahrad, R., Saljoughian, M., & Kafi, M. A. (2019). Experimental evaluation of RC frames retrofitted by steel jacket, X-brace and X-brace having ductile ring as a structural member. *Journal of Building Pathology and Rehabilitation, 4*(1), 11.

Krawinkler, H. (1992). Guidelines for cyclic seismic testing of components of steel structures for buildings. *Report No. ATC-24, Applied Technology Council, Redwood City, CA*.

Lian, M., Su, M., & Guo, Y. (2015). Seismic performance of eccentrically braced frames with high strength steel combination. *Steel and Composite Structures, 18*(6), 1517–1539.

Liang, C., Qian, C., Chen, H., & Kang, W. (2018a). Prediction of compressive strength of concrete in wet-dry environment by BP artificial neural networks. *Advances in Materials Science and Engineering, 2018*.

Liang, C., Qian, C., Chen, H., & Kang, W. (2018b). Prediction of compressive strength of concrete in wet-dry environment by BP artificial neural networks. *Advances in Materials Science and Engineering, 2018*, 11. https://doi.org/10.1155/2018/6204942.

Ling, H., Qian, C., Kang, W., Liang, C., & Chen, H. (2019). Combination of support vector machine and K-fold cross validation to predict compressive strength of concrete in marine environment. *Construction and Building Materials, 206,* 355–363.

Mazzoni, S., McKenna, F., Scott, M. H., & Fenves, G. L. (2006). The open system for earthquake engineering simulation (OpenSEES) user command-language manual.

Menegotto, M. (1973). Method of analysis for cyclically loaded RC plane frames including changes in geometry and non-elastic behavior of elements under combined normal force and bending. In *Proceedings of IABSE symposium on resistance and ultimate deformability of structures acted on by well defined repeated loads* (pp. 15–22)

Naghavi, M., Rahnavard, R., Thomas, R. J., & Malekinejad, M. (2019). Numerical evaluation of the hysteretic behavior of concentrically braced frames and buckling restrained brace frame systems. *Journal of Building Engineering, 22,* 415–428.

Okazaki, T. (2004). Seismic performanc of link-to-column connections in steel eccentrically braced frames (Doctoral dissertation). The University of Texas at Austin. USA.

Pachideh, G., Gholhaki, M., & Kafi, M. (2020). Experimental and numerical evaluation of an innovative diamond-scheme bracing system equipped with a yielding damper. *Steel and Composite Structures, 36*(2), 197–211.

Prinz, G., & Richards, P. (2009). Eccentrically braced frame links with reduced web sections. *Journal of Constructional Steel Research, 65*(10–11), 1971–1978.

Rahnavard, R., Hassanipour, A., Suleiman, M., & Mokhtari, A. (2017). Evaluation on eccentrically braced frame with single and double shear panels. *Journal of Building Engineering, 10,* 13–25.

Rahnavard, R., Rebelo, C., Craveiro, H. D., & Napolitano, R. (2020). Numerical investigation of the cyclic performance of reinforced concrete frames equipped with a combination of a rubber core and a U-shaped metallic damper. *Engineering Structures, 225,* 111307.

Ramadan, T., & Ghobarah, A. (1995). Analytical model for shear-link behavior. *Journal of Structural Engineering, 121*(11), 1574–1580.

Richards, P. W. (2004). *Cyclic stability and capacity design of steel eccentrically braced frames*. San Diego: University of California.

Salimbahrami, S. R. (2013). *The role of ductility behavior of connection elements on seismic assessments of EBF*. Babol: Babol Noshirvani University of Technology.

SAP, C. (2005). *Structural analysis program*. Berkeley: California.

Stolarski, T., Nakasone, Y., & Yoshimoto, S. (2018). *Engineering analysis with ANSYS software*. Oxford: Butterworth-Heinemann.

UBC. (1994). Structural engineering design provisions, Uniform Building Code, Vol. 2. In *International Conference of Building Officials, 1994*